Evaluation of Hydraulic Efficiency of Disinfection Systems Based on Residence Time Distribution Curves

JORDAN M. WILSON AND SUBHAS K. VENAYAGAMOORTHY*

Department of Civil and Environmental Engineering, Colorado State University, 1372 Campus Delivery, Fort Collins, Colorado 80523-1372, United States

Received August 19, 2010. Revised manuscript received November 2, 2010. Accepted November 9, 2010.

Hydraulic efficiency is a vital component in evaluating the disinfection capability of a contact system. Current practice evaluates these systems based upon the theoretical detention time (*TDT*) and the rising limb of the residence time distribution (RTD) curve. This evaluation methodology is expected because most systems are built based on *TDT* under a "black-box" approach to disinfection system design. Within recent years, the proliferation of computational fluid dynamics (CFD) has allowed a more insightful approach to disinfection system design and analysis. Research presented in this study using CFD models and physical tracer studies shows that evaluation methods based upon *TDT* tend to overestimate, severely in some instances, the actual hydraulic efficiency as obtained from the system's flow and scalar transport dynamics and subsequent RTD curve. The main objective of this study was to analyze an alternative measure of hydraulic efficiency, the ratio t_{10}/t_{90}, where t_{10} and t_{90} are the time taken for 10 and 90% of the input concentration to be observed at the outlet of a system, respectively, for various disinfection systems, primarily a pipe loop system, pressurized tank system, and baffled tank system, from their respective RTD curves and compare the results to the current evaluation method.

Introduction

Hydraulic efficiency is an important component in the design and operation of disinfection systems, particularly chlorine contact tanks, considering the potential carcinogenic products formed in the chlorination process. Improving the hydraulic efficiency of a system allows for a smaller dose of disinfectant to be used thus reducing the formation of potential carcinogens (*1, 2*). Until recently contact tanks used in water treatment have been largely regarded as "black boxes" and their design left up to the ideal assumption of plug flow, that is, the theoretical detention (or residence) time (*TDT*) of the system is simply the ratio of the system volume, *V*, to the average volumetric flow rate, *Q* (*3*−*5*). The reality is that very few contact tanks function in a strictly plug flow manner (further details can be found in ref *6*). Most contact tanks have an uneven flow path, inducing regions of recirculation or stagnation, commonly known as dead zones (*5*). These dead zones rely on the much slower process of diffusion to distribute the disinfectant, causing particles in the contact tank to reside longer than the *TDT*. The problem with the *TDT* formulation is that this value is a prediction based on idealized plug flow conditions rather than the actual flow dynamics of the tank. The further the flow in the tank departs from plug flow (e.g., the more recirculation, turbulence, and stagnation fluid particles encounter), the further the actual detention time is from the *TDT* (*3*).

In order to evaluate the efficiency of contact tanks for disinfection purposes, the United States Environmental Protection Agency (USEPA) has established the practice of assigning tanks a baffle factor (*BF*) (*7*). The contact time of the disinfectant with the water in the tank is taken to be t_{10}, which is the time for 10% of the inlet concentration to be observed at the outlet. These quantities are typically obtained through tracer studies of an established system using conductivity measurements or tracer analysis using fluoride or lithium. *BF* is the ratio of t_{10} to *TDT* and ranges from a value of 0.1 representing an unbaffled tank with significant short-circuiting to an upper bound value of 1.0 representing ideal plug flow conditions as described by the Interim Enhanced Surface Water Treatment Rule (*7*). In addition, the Morrill Index (*MI*), used as a measure of hydraulic efficiency in Europe, evaluates the amount of diffusion in a system based on the ratio t_{90}/t_{10} (*6, 8*). The USEPA's practice of assigning *BFs* assumes that a system can achieve plug flow through the use of *TDT*s. However, advances in numerical analysis and computational fluid dynamics (CFD) allow for a more comprehensive understanding into the flow dynamics of a system. The research presented in this paper shows that a better measure of hydraulic efficiency must include the complete flow dynamics of the system since it is the flow dynamics that governs the transport of a tracer from the inlet to outlet through time (*9*). This is usually depicted by a residence time distribution (RTD) or flow through curve (FTC), obtained by plotting the system's effluent concentration over time, as shown for example in Figure 1.

The shape of the RTD curve provides insight to the nature of the flow in the system (*10*). For example, a steeper gradient represents conditions closer to plug flow dominated by advective forces and a flatter gradient represents conditions further from plug flow dominated by diffusive forces. The RTD curve shows the complete interaction of the scalar (e.g., chlorine-containing species) and fluid flow field (*9*), thus, it should be used in its entirety to evaluate hydraulic efficiency. However, current practice only uses the rising limb, or rather the t_{10} value, from the RTD curve and compares it to a *TDT* value unrelated to the actual flow in the system. This

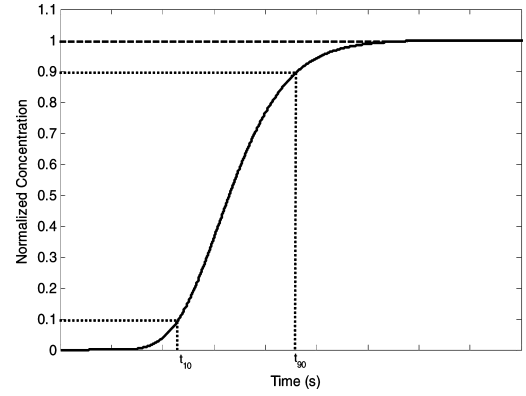

FIGURE 1. Residence time distribution (RTD) curve for an arbitrary disinfection system.

* Corresponding author phone: (970)491-1915; fax: (970)491-7727; e-mail: vskaran@engr.colostate.edu.

methodology often leads to a *BF* that overestimates the system's actual hydraulic efficiency, as shown throughout the results in this study.

In what follows, a brief overview of the numerical modeling and physical experiments used in this study is provided. Three chlorine contact systems, a pipe loop contactor, a series of pressurized tanks, and a baffled contact tank (*11*), were evaluated using CFD with a scalar transport model to determine their respective hydraulic efficiencies. The pipe loop contactor and pressurized tank system (designated as disinfection systems by the Water Quality Division of The Colorado Department of Public Health and Environment) were also evaluated with tracer studies to provide validation for the CFD models. The results of these evaluation methods are finally discussed in detail, providing the basis for a better evaluation methodology of hydraulic efficiency based on the ratio of t_{10} to t_{90} obtained from the RTD curves.

Theoretical Basis

Flow Modeling and Scalar Transport. For purposes of this study, the chemical and biological processes of disinfection within contact tanks were not considered because of the relatively short residence times. This study focused on the efficiency with which a passive scalar is mixed throughout the system. A passive scalar is any species that can be transported but is nonreactive and has no influence on the flow field. Traditionally such studies have been performed on Froude scale models; however, Falconer and Liu (*12*) showed that physical models often overestimate the advection-diffusion processes and momentum transfer and underestimate the influences of bed friction. Advances in numerical modeling and CFD allow for the analysis of a full-scale model while being cost-effective and adaptable (*13, 14*). A time-averaged solution was utilized by solving the Reynolds Averaged Navier−Stokes (RANS) equations with a standard k-ε turbulence model (for details, see e.g. ref *15*) for the systems. The transport of a passive scalar (e.g., a conservative tracer) is governed by the advection-diffusion equation given by

$$\frac{DC}{Dt} = \frac{\partial C}{\partial t} + \bar{U}.\nabla C = \nabla\cdot\left(\left(\kappa + \frac{\upsilon_t}{Sc_t}\right)\nabla C\right) \qquad (1)$$

where C is the concentration (e.g., chlorine-containing species or lithium), $\bar{U}$ is the steady state turbulent velocity field, κ is the molecular diffusivity of the tracer, ν_t is the turbulent eddy viscosity, and Sc_t is the turbulent Schmidt number. $\bar{U}$ and ν_t are obtained from the steady state solution of the momentum equations. For neutrally stratified flows as in this study, the turbulent Schmidt number Sc_t is taken as 0.7 (for justification, see e.g. ref *16*).

CFD Model Methodology. ANSYS Workbench v. 12.0 was used for the preprocessing development of the computational model. The CFD software FLUENT v. 12.1, a finite volume code, developed by ANSYS was used to solve the computational model and for postprocessing analysis. Within FLUENT, the computational model was first run to steady state to ensure a converged velocity field. Second, the steady state velocity field was used to initialize a transient model to solve for the passive scalar concentration field as it passed through the system. The scalar concentration was monitored at the outlet of the system to produce the RTD curve for the system. Because the scalar concentration was set to a maximum nondimensional concentration of 1, the values of t_{10} and t_{90} could be easily interpreted from the RTD curve. Grid independence was performed for each of the computational models to ensure solution convergence.

Physical Experiment Methodology. Step-dose tracer studies were performed on the pipe loop and pressurized tank systems. Lithium was selected as a tracer because of its conservative nature and extremely low background levels found in the raw water. A stock solution of lithium chloride (LiCl) and water was mixed such that the maximum concentration observed in the effluent of the systems would be approximately 0.04 mg/L. Samples were taken based on the RTD curve produced from the CFD model and analyzed at the Soil, Water, and Plant Testing Laboratory at Colorado State University using inductively coupled plasma-atomic emission spectroscopy.

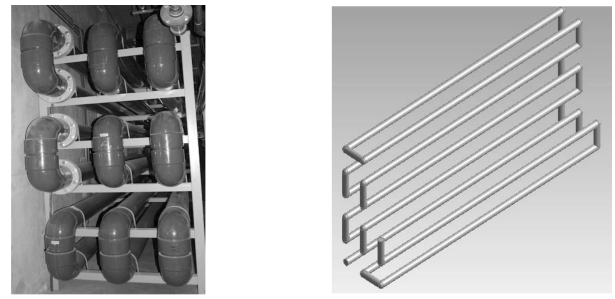

FIGURE 2. (a) Pilot pipe-loop facility at Fort Collins Water Treatment Facility and (b) pipe loop geometry for CFD analysis.

Experimental Methods

The following subsections describe the three disinfection systems analyzed in this study. A pipe loop contactor and system of pressurized tanks were evaluated using CFD models with a scalar transport model and physical tracer studies to determine their respective hydraulic efficiency. A baffled contact tank system (*11*) was evaluated as a case study based on the work of Xu and Venayagamoorthy (*17*).

Pipe Loop System Configuration. The city of Fort Collins Municipal Water Treatment Facility allowed the use of their pilot pipe loop system for this study. The pipe loop facility had a total of 18 lengths, but the tracer was sampled after 14 lengths to take advantage of a pre-existing tap in the system. The internal diameter of the piping was 0.15 m. The pipe-loop had a major length of 6.55 m and a minor length of 0.21 m measured from the outside of the joints. Figure 2(a) shows the pilot pipe-loop facility, while Figure 2(b) shows the model geometry reflecting the sampling point after 14 lengths containing 895,950 tetrahedral cells on an unstructured grid.

Pressurized Tank System Configuration. This system was designed and constructed at Colorado State University's hydraulics laboratory. The pressurized tank system was constructed using industry standard 0.3 m^3 fiberglass tanks connected using 0.03175 m diameter schedule 80 PVC pipe and plumbed in a manner that allowed multiple flow arrangements to be analyzed without altering the footprint of the system. The system was analyzed for one, two, and three tanks in series, respectively. Figure 3(a) shows the pressurized tank system, while Figure 3(b) shows the model geometry reflecting the system setup in a series configuration containing approximately 2,104,000 tetrahedral cells on an unstructured grid.

Baffled Tank System Configuration. The analyzed system was based on the pilot scale experimental study of a contact tank by Shiono et al. (*11*) with a length of 1.995 m, a width of 0.94 m, and seven internal baffles each measuring 0.75 m in length. To further investigate the hydraulic efficiency characteristics of the system, Xu and Venayagamoorthy (*17*) altered the number of baffles, from zero to ten, on the same footprint as the pilot tank used by Shiono et al. (*11*).

Results

Pipe Loop System. The tracer study analyzed flow rates of 0.000505 and 0.001093 m^3/s (or 8 and 16 gallons per minute

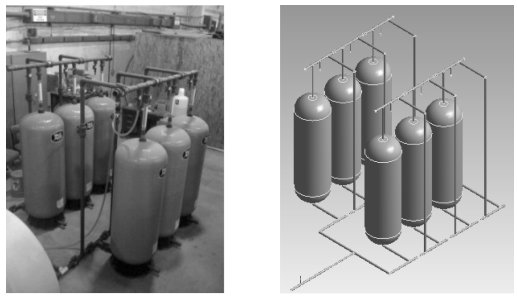

(a) (b)

FIGURE 3. (a) Full-scale series tank configuration and (b) series tank configuration for CFD analysis.

TABLE 1. Results of CFD Model and Tracer Study Analysis of Pilot Pipe-Loop Facility

analysis	Q (m^3/s)	t_{10} (s)	t_{90} (s)	TDT (s)	BF	t_{10}/t_{90}
CFD model	0.000505	3234	3774	3360	0.96	0.86
	0.001093	1584	1890	1680	0.94	0.84
tracer study	0.000505	3120	3786	3360	0.93	0.82
	0.001093	1536	1950	1680	0.91	0.79

(gpm) in English units), respectively. Table 1 presents the results of the pipe loop analysis which show that the BF values are consistently higher than the t_{10}/t_{90} values by approximately 10%.

Figures 4(a) and 4(b) show a comparison of RTD curves for the tracer study and CFD model results for two different flow rates. The CFD model and lithium tracer RTD curves correlated closely, as observed in Figures 4(a) and 4(b), thus validating the CFD analysis for three-dimensional scalar transport on the specified pipe-loop configuration.

Pressurized Tank System. The tracer study analyzed flow rates of 0.000631, 0.000946, and 0.001262 m^3/s (or 10, 15, and

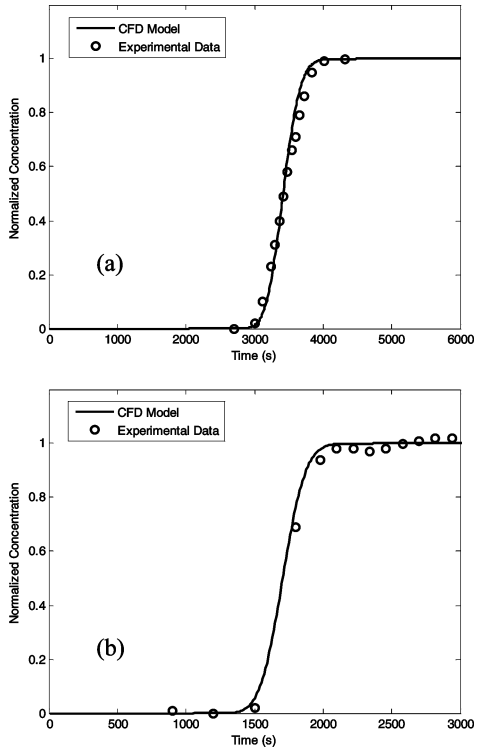

FIGURE 4. Comparison of CFD model and tracer study RTD curves for pipe loop facility for (a) 0.000505 m^3/s and (b) 0.001093 m^3/s.

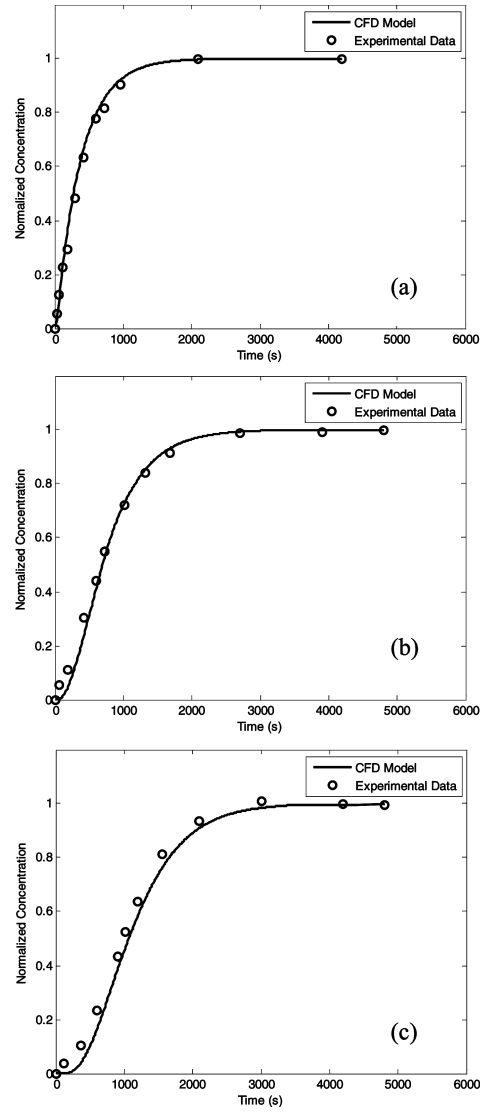

FIGURE 5. Comparison of CFD model and tracer study RTD curves for 0.000946 m^3/s (15 gpm) through (a) one tank, (b) two tanks, and (c) three tanks in series.

20 gpm) for one, two, and three tanks in series, respectively. Figures 5 (a), (b), and (c) show the comparison of RTD curves for the tracer study and the CFD model results for one, two, and three tanks in series at a flow rate of 0.000946 m^3/s (15 gpm), respectively. The CFD model and lithium tracer RTD curves again correlated closely, as observed in Figures 5(a), (b), and (c), thus validating the CFD analysis for three-dimensional scalar transport on the specified pressurized tank configuration.

Table 2 shows the data resulting from the series tank system analysis. Again, the results presented in Table 2 show that the BF values are consistently higher than the t_{10}/t_{90} values.

Figures 6(a) and 6 (b) show the hydraulic efficiency versus the number of tanks in series over the system for the CFD models and tracer studies, respectively.

Figures 6(a) and 6(b) also show a linear regression curve fit to each series of data points and their corresponding equations and coefficients of determination, R^2, with a y-intercept of zero. Despite the differences in the BF and t_{10}/t_{90} values of the computational model and tracer study results, the curve fits in Figures 6(a) and 6 (b) show a linear scale-up in the hydraulic efficiency with an increase of the number of tanks (N_T) in series. Furthermore, Figures 6(a)

TABLE 2. Results of CFD Model and Tracer Study Analysis of Series Tank System

analysis	no. of tanks in series, N_T	Q (m^3/s)	t_{10} (s)	t_{90} (s)	TDT (s)	BF	t_{10}/t_{90}
CFD model	1	0.000631	108	1212	498	0.21	0.09
	1	0.000946	60	870	336	0.19	0.07
	1	0.001262	54	624	252	0.22	0.09
	2	0.000631	354	2106	1002	0.36	0.17
	2	0.000946	252	1506	666	0.38	0.17
	2	0.001262	210	1062	498	0.42	0.20
	3	0.000631	744	3078	1500	0.50	0.24
	3	0.000946	498	2046	1002	0.50	0.24
	3	0.001262	378	1548	750	0.50	0.24
tracer study	1	0.000631	48	1266	498	0.10	0.04
	1	0.000946	48	948	336	0.14	0.05
	1	0.001262	30	684	252	0.12	0.04
	2	0.000631	300	2496	1002	0.30	0.12
	2	0.000946	162	1608	666	0.24	0.10
	2	0.001262	168	1110	498	0.34	0.15
	3	0.000631	510	3048	1500	0.34	0.17
	3	0.000946	354	1944	1002	0.35	0.18
	3	0.001262	258	1530	750	0.34	0.17

and 6(b) show that the BF values overestimate the hydraulic efficiency described by t_{10}/t_{90} by approximately 100% for both cases.

Baffled Tank System. Figures 7(a)-(d) show the contours of velocity magnitude (in m s^{-1}) for the internal baffle configurations. As the number of baffles increased in the system, the area of the dead zones decreased. The values of BF and t_{10}/t_{90} reflect this observation as show in Table 3. The efficiency of the baffled tank system increases in a manner that appears to never reach plug flow conditions regardless of the number of baffles. Further details on the hydraulic efficiency of baffled tanks are discussed by Xu and Venayagamoorthy (*17*).

Figure 8 shows the RTD curves of the internal baffle configurations (from zero to ten) of the pilot scale chlorine contact tank shown in part in Figures 7(a)-(d). The gradient of the RTD curve increases with the number of baffles, indicating that advective transport begins to dominate diffusive transport as the number of baffles increases in the tank.

Table 3 presents the results of the two-dimensional CFD analysis of the varying internal baffle configurations of the chlorine contact tank. The results clearly show that the BF is consistently greater than the quantity t_{10}/t_{90} even for the two-dimensional simulations used in this specific configuration.

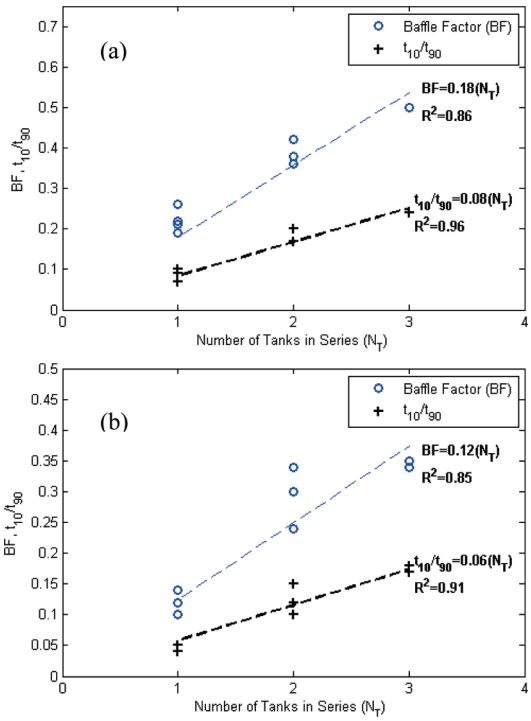

FIGURE 6. Comparison of BF and t_{10}/t_{90} values for (a) CFD model and (b) tracer study.

Discussion

While estimates can be made about a systems efficiency based on the BF guidelines (*6*), a tracer study and resulting

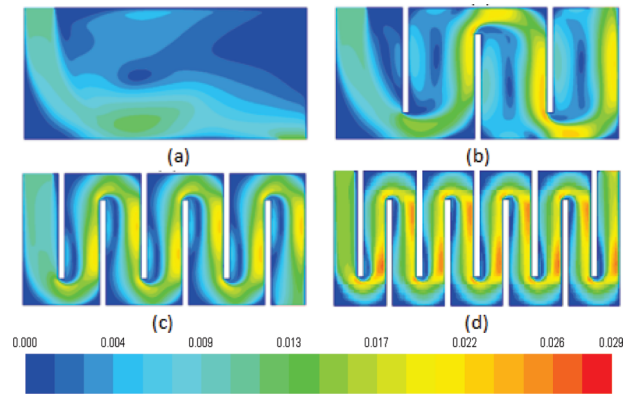

FIGURE 7. Contours of velocity magnitude (in m s^{-1}) for pilot scale chlorine contact tank with (a) zero, (b) three, (c) six, and (d) nine internal baffles (*17*).

TABLE 3. Results of CFD Analysis for Pilot Scale Contact Tank of Varying Internal Baffle Configurations

no. of baffles	V (m^3)	Q (m^3/s)	TDT (s)	t_{10} (s)	t_{90} (s)	BF	t_{10}/t_{90}
0	1.0052	0.0012	859.11	258	1923	0.30	0.13
1	0.9871	0.0012	843.65	275	2373	0.33	0.12
2	0.9690	0.0012	828.19	294	1980	0.36	0.15
3	0.9509	0.0012	812.73	349	1793	0.43	0.19
4	0.9328	0.0012	797.27	415	1484	0.52	0.28
5	0.9147	0.0012	781.80	498	1295	0.64	0.38
6	0.8966	0.0012	766.34	597	1182	0.78	0.51
7	0.8785	0.0012	750.88	617	1080	0.82	0.57
8	0.8604	0.0012	735.42	617	1015	0.84	0.61
9	0.8424	0.0012	719.96	623	958	0.86	0.65
10	0.8243	0.0012	704.50	623	926	0.88	0.67

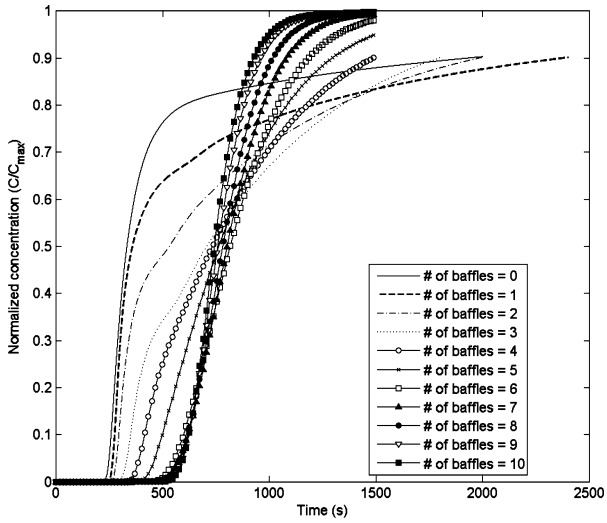

FIGURE 8. Comparison of RTD curves for internal baffle configurations of pilot scale chlorine contact tank.

RTD curve or combination of a CFD model and validation tracer study are the only ways to evaluate the respective hydraulic efficiencies of the systems. As seen in this study, even the detention time in a pipe loop, listed as a perfect plug flow contactor by the USEPA, departs from a perfect step function. A full RTD curve is a clear indicator of the internal flow dynamics of a system; whether it be a short-circuited flow, plug flow, or somewhere in between (*10, 18*). There are many contributing factors for this departure of the flow such as boundary layer turbulence, flow separation, entry and exit conditions, and buoyancy forces due to stratification. As a result, the t_{10}/t_{90} values for all three systems discussed in this study are consistently lower than the values for the *BF*. Because the *BF* formulation assumes that a perfect plug flow can be achieved in every system, it, therefore, inherently overestimates the hydraulic efficiency. For example, systems of the same volume can have differing geometries yet have the same *TDT* for a given flow rate. Clearly, large unbaffled rectangular tanks and long pipe contactors have differing flow dynamics and should not have their efficiencies evaluated based on the same idealized *TDT,* which assumes plug flow conditions.

Because a disinfection system with a sufficiently large length-to-width ratio asymptotically approaches ideal plug flow behavior, the *BF* values did not differ as significantly from the t_{10}/t_{90} values in the pipe loop contactor as they did in the pressurized and baffled tank systems. As the length-to-width ratio decreases, the difference in *BF* and t_{10}/t_{90} values increases due to diffusion and other flow phenomena (e.g., flow separation and recirculation). This also results in a further departure from the ideal plug flow assumption inherent in the *BF* formulation of a purely advective system. Furthermore, the results of the CFD models and tracer studies suggest that the ratio of t_{10} to t_{90} is a more appropriate measure of hydraulic efficiency. The values of t_{10} and t_{90} are obtained from the RTD curve which as previously mentioned is a direct indicator of the flow dynamics in the system, thus eliminating any ambiguity associated with the *TDT*. The *MI* evaluates the amount of diffusion in a system based on the ratio t_{90}/t_{10} with a lower bound value of 1.0 representing pure advection (ideal plug flow) but is convoluted in that there is no upper limit to describe the amount of diffusion in the system (*3*). In contrast, the quantity t_{10}/t_{90} gives the ratio of advective to diffusive actions with an upper bound value of 1.0 representing pure advection and a lower bound value of zero representing (at least in theory) pure diffusion. In this manner, t_{10}/t_{90} presents a straightforward ratio from which one can easily deduce the influence of advective and diffusive forces on the system similar to the Peclet number which is a measure of the advection to diffusion effects in a fluid transport system and is given by

$$Pe = \frac{UL}{\kappa} \tag{2}$$

where U is a characteristic velocity scale of the flow, L is a characteristic length scale, and κ is the molecular diffusivity. A high Peclet number would imply a system which is dominated by advection and vice versa for a system dominated by diffusion. Hence, the ratio of t_{10}/t_{90} can in fact be considered as a form of the Peclet number expressed here as a time scale ratio.

As with any disinfection system, a more efficient system requires less contact time for a given amount of chlorine-containing species to achieve a certain level of log-inactivation. While the USEPA guidelines have proven adequate for use in contact tank systems, this study has shown that *BFs* only provide a partial assessment of the hydraulic efficiency, making use of only the rising limb of the RTD curve, and thus tend to overestimate the hydraulic efficiency of the disinfection system. On the other hand, the t_{10}/t_{90} ratio provides a better measure of the hydraulic efficiency of any disinfection system since it takes into account the actual flow and scalar transport dynamics in a given system by utilizing a substantial portion of the RTD curve of a given system.

Acknowledgments

Grateful acknowledgment is given to the Colorado Department of Public Health and Environment (CDPHE) Water Quality Division, USA (Program Engineers: Tyson Ingels, Melanie Criswell, Gordon Whittaker, and Sharon Williams) for their support on this project. We also thank the Fort Collin Water Treatment Facility (Water Production Manager: Lisa Voytko, and Ken Morrison) for the use of their pilot pipe-loop facility. Qing Xu graciously provided her data and figures for the baffled tank system.

Literature Cited

(1) Singer, P. C. Control of disinfection by-products in drinking water. *J. Environ. Eng.* **1994**, *120* (4), 727–744.
(2) Wang, H.; Shao, X.; Falconer, R. A. Flow and transport simulation models for prediction of chlorine contact flow-through curves. *Water Res.* **2003**, *75* (5), 455–471.
(3) Kothandaraman, V.; Southerlan, H. L.; Evans, R. L. Performance characteristics of chlorine contact tanks. *J. - Water Pollut. Control Fed.* **1973**, *45* (4), 611–619.
(4) Shiono, K.; Teixeira, E. C. Turbulent characteristics in a baffled contact tank. *J. Hydraul. Res.* **2000**, *38* (4), 271–271.
(5) Wang, H.; Falconer, R. A. Simulating disinfection processes in chlorine contact tanks using various turbulence models and high-order accurate difference schemes. *Water Res.* **1998**, *32* (5), 1529–1543.
(6) United States Environmental Protection Agency, USEPA. Design manual: municipal wastewater disinfection; EPA:625:1-86:021; USEPA Office of Res. and Dev.: Cincinnati, OH, 1986.
(7) United States Environmental Protect Agency, USEPA. Disinfection profiling and benchmarking guidance manual; EPA 815-R-99-013; Office of Water: Washington, DC, 2003.
(8) Teixeira, E.; Siqueira, R. Performance Assessment of Hydraulic Efficiency Indexes. *J. Environ. Eng.* **2008**, *134* (10), 851–859.
(9) Stamou, A. I.; Noutsopoulos, G. Evaluating the Effect of Inlet Arrangement in Settling Tanks Using the Hydraulic Efficiency Diagram. *Water SA* **1994**, *20* (1), 77–83.
(10) Stamou, A. I. Verification and application of a mathematical model for the assessment of the effect of guiding walls on hydraulic efficiency of chlorination tanks. *J. Hydroinformatics* **2002**, *4*, 245–254.

(11) Shiono, K. E.; Teixiera, E. C.; Falconer, R. A. *Turbulent measurements in chlorine contact tank*, The 1st international conference on water pollution: Modeling, measuring, and predicting, Southampton, UK, 1991; pp 519−531.
(12) Falconer, R. A.; Liu, S. Modeling solute transport using QUICK scheme. *J. Environ. Eng.* **1998**, *114* (1), 3–20.
(13) Falconer, R. A.; Ismail, A. I. B. M. Numerical modeling of tracer transport in a contact tank. *Environ. Int.* **1997**, *23* (6), 763–773.
(14) Stamou, A. I. Improving the hydraulic efficiency of water process tanks using CFD models. *Chem. Eng. Process.* **2008**, *47*, 1179–1189.
(15) Pope, S. B. *Turbulent Flows*; Cambridge University Press: Cambridge, U.K., 2000.
(16) Venayagamoorthy, S. K.; Stretch, D. D. On the turbulent Prandtl number in homogeneous stably stratified turbulence. *J. Fluid Mech.* **2010**, *644*, 359–369.
(17) Xu, Q.; Venayagamoorthy, S. K. *Hydraulic efficiency of baffled disinfection contact tanks*, 6th International Symposium on Environmental Hydraulics, 23−25 June 2010, Athens, 2010; pp 1041−1046.
(18) Lyn, D. A.; Rodi, W. Turbulent measurements in model settling tank. *J. Hydraul. Eng.* **1990**, *116* (1), 3–21.

ES102861G